

Field-effect transistors as electrically controllable nonlinear rectifiers for the characterization of terahertz pulses

Alydas Lisauskas, Kęstutis Ikamas, Sylvain Massabeau, Maris Bauer, Dovilė Čibiraitė, Jonas Matukas, Juliette Mangeney, Martin Mittendorff, Stephan Winnerl, Viktor Krozer, and Hartmut G. Roskos

Citation: *APL Photonics* **3**, 051705 (2018); doi: 10.1063/1.5011392

View online: <https://doi.org/10.1063/1.5011392>

View Table of Contents: <http://aip.scitation.org/toc/app/3/5>

Published by the [American Institute of Physics](#)

STEM CAREER WEBINARS

on networking, interviewing,
conferences, presenting...

www.physicstoday.org/jobs/webinars



Field-effect transistors as electrically controllable nonlinear rectifiers for the characterization of terahertz pulses

Alvydas Lisauskas,^{1,2,a} Kęstutis Ikamas,¹ Sylvain Massabeau,³ Maris Bauer,² Dovilė Čibiraite,² Jonas Matukas,¹ Juliette Mangeney,³ Martin Mittendorff,⁴ Stephan Winnerl,⁴ Viktor Krozer,² and Hartmut G. Roskos²

¹*Institute of Applied Electrodynamics and Telecommunications, Vilnius University, Sauletekio Ave. 3, LT-10257 Vilnius, Lithuania*

²*Physikalisches Institut, Goethe-Universität Frankfurt, Max-von-Laue-Str. 1, D-60438 Frankfurt am Main, Germany*

³*Laboratoire Pierre Aigrain, Ecole Normale Supérieure-PSL Research University, CNRS, Université Pierre et Marie Curie-Sorbonne Universités, Université Denis Diderot-Sorbonne Paris Cité, 24 rue Lhomond, 75231 Paris Cedex 05, France*

⁴*Helmholtz-Zentrum Dresden-Rossendorf, Dresden DE-01328, Germany*

(Received 31 October 2017; accepted 17 February 2018; published online 7 March 2018)

We propose to exploit rectification in field-effect transistors as an electrically controllable higher-order nonlinear phenomenon for the convenient monitoring of the temporal characteristics of THz pulses, for example, by autocorrelation measurements. This option arises because of the existence of a gate-bias-controlled super-linear response at sub-threshold operation conditions when the devices are subjected to THz radiation. We present measurements for different antenna-coupled transistor-based THz detectors (TeraFETs) employing (i) AlGaIn/GaN high-electron-mobility and (ii) silicon CMOS field-effect transistors and show that the super-linear behavior in the sub-threshold bias regime is a universal phenomenon to be expected if the amplitude of the high-frequency voltage oscillations exceeds the thermal voltage. The effect is also employed as a tool for the direct determination of the speed of the intrinsic TeraFET response which allows us to avoid limitations set by the read-out circuitry. In particular, we show that the build-up time of the intrinsic rectification signal of a patch-antenna-coupled CMOS detector changes from 20 ps in the deep sub-threshold voltage regime to below 12 ps in the vicinity of the threshold voltage. © 2018 Author(s). All article content, except where otherwise noted, is licensed under a Creative Commons Attribution (CC BY) license (<http://creativecommons.org/licenses/by/4.0/>). <https://doi.org/10.1063/1.5011392>

Utilization of sources generating short optical pulses requires techniques for the monitoring of the temporal characteristics of the pulses. The monitoring is often performed by an interferometric autocorrelation technique with detectors which possess higher-order nonlinearity.¹ In the optical and mid-infrared spectral domains, one often employs quadratic detection exploiting two-photon absorption or sum-frequency generation. In the THz frequency domain, finding convenient detectors for the monitoring of pulsed sources remains to be a challenge. One option is quantum-engineered devices, exploiting, for example, intersubband transitions, but due to the low THz photon energy, such detectors require cryogenic cooling.^{2,3} Here, we propose to exploit electrical rectification in field-effect transistors (FETs) which provide electrically controllable higher-order nonlinearities and temporal resolution on a picosecond scale. The detectors can be operated at room temperature.

Since the initial proposal to utilize FETs for the detection of THz radiation,⁴ there was a continuous development both in achieved performance and in the theoretical understanding of the underlying rectification phenomenon. On the theory side, it was recognized that the plasmonic description

^aElectronic mail: alvydas.lisauskas@ff.vu.lt



of carrier dynamics in the channel is equivalent to wave propagation on a nonlinear transmission line (TL).⁵⁻⁸ Analytical models have been extended to cover both the sub-threshold and inversion regimes.⁹ Furthermore, TL-based theories have been modified to account for the nature of electron screening at comparatively large wavevectors k for $kd \geq 1$ with d being the separation between the gate electrode and the channel.^{10,11} TL-based theories now are able to predict responses to low-intensity radiation with a seamless extension to high intensities¹² and implementation in standard circuit simulation programs.¹³

TeraFETs have been employed for the detection of (sub-)nanosecond THz pulses taking advantage of the fact that the build-up time of their response is in the range of only ten or a few tens of picoseconds.¹⁴⁻¹⁶ Theory predicts that at low excitation powers, FET detectors are linear power detectors, whereas for high excitation levels, the output signal saturates. The predictions have been validated for different material systems¹⁷ as well as for different biasing regimes.^{12,18} The saturation behavior of TeraFET detectors has been used for autocorrelation measurements to monitor the duration of THz pulses.¹⁹

An interesting observation has recently been reported that AlGaIn/GaN transistors at sub-threshold gate bias, if illuminated by sub-nanosecond THz pulses, exhibit a super-linear response slope before reaching saturation.²⁰ The authors have suggested that this phenomenon could be explained by a change of the conductivity value during the pulse, most probably related to trapping states in AlGaIn.²¹

Here, we experimentally investigate this super-linear response at sub-threshold bias conditions and find it for both AlGaIn/GaN high-electron-mobility transistors and silicon CMOS FETs subjected to THz pulses. We explore the dynamic range over which it occurs and theoretically show that a super-linear response is a universal property of rectification at low gate bias voltage for high radiation intensities just before saturation sets in. We show that the phenomenon can be exploited for the temporal diagnostics of THz pulses as well as for the determination of the intrinsic response time of the FET avoiding limitations set by the read-out electronics.

For the investigation of the detector response, we employed two THz radiation sources: (i) the first one was a photoconductive antenna driven tens-of-femtosecond-long infrared pulses from a Ti:sapphire laser system with a pulse compressor and (ii) the second one was the free-electron-laser THz source FELBE at the Helmholtz-Zentrum Dresden Rossendorf. The TeraFETs were operated at zero source-drain bias.

In the first case, we used a THz time-domain spectroscopy system for the measurements. It employs a 80-MHz-repetition-rate pulse train centered at a wavelength of 800 nm, delivered by a Ti:sapphire oscillator followed by a fiber-based pulse compressor.²² The optical pulses, with a 15-47-fs-long adjustable duration and a pulse energy of 4 nJ, illuminate a large-area interdigitated photoconductive antenna to generate THz pulses.²³ The photoconductive antenna consists of metallic electrodes with 2- μm wide and 2- μm spaced fingers on a 1- μm thick low-temperature-grown GaAs layer on a semi-insulating GaAs wafer. Every second period of the metal-semiconductor-metal finger structure is masked by a second metal pattern (Cr-Au), electrically isolated from the first one by a SiO₂ layer of 560-nm thickness, to ensure that at each optically excited spot of the emitter, THz radiation is generated with a common polarization direction.²⁴ The antenna surface is 500 \times 500 μm^2 . The antenna was biased by a 0-10-V peak-to-peak square wave which was modulated at 10 kHz. The emitted THz radiation was first collimated and then focused with two off-axis paraboloidal mirrors (f-number of 2) to a diffraction-limited spot on a broad-band antenna-coupled AlGaIn/GaN HEMT TeraFET detector. A Teflon filter was placed into the beam between the paraboloidal mirrors to block residual laser radiation. The detector's response was measured using a lock-in technique employing either voltage or current input. The TeraFET was fabricated at the Ferdinand-Braun-Institute (FBH) using a GaN Monolithic Microwave Integrated Circuit (MMIC) process on SiC substrate.^{25,26} The HEMT had a gate length of 0.1 μm . Asymmetric radiation coupling, required for efficient detection, was realized by a capacitive coupling at the gate and source terminals via a metal-insulator-metal (MIM) capacitance, using the gate and source contact metal layers, respectively.²⁷ With this approach, the THz radiation excites plasma waves at the drain side of the transistor only. A hyper-hemispherical silicon lens was used to further enhance in-coupling of THz radiation.²⁶ The device exhibited a minimal noise-equivalent power (NEP) of 31 pW/ $\sqrt{\text{Hz}}$ at a frequency of 600 GHz, with the NEP

remaining below $100 \text{ pW}/\sqrt{\text{Hz}}$ between 350 GHz and 1.2 THz. The THz pulses had a spectral extent from 0.1 THz to 2.5 THz (10-% points of the power spectrum).

In the second case, we employed the FELBE radiation source, one of the free-electron lasers (FELs) at the Forschungszentrum Dresden-Rossendorf, Germany. The laser was operated in the continuous 13-MHz pulsing mode with a pulse duration in the range of 10-25 ps. The average power reached about 10 W and was attenuated with built-in calibrated attenuation sheets. The spatial intensity distribution was recorded with a pyroelectric camera (Pyrocam III). At 4.3 THz, the measured full-width at half maximum (FWHM) of the cross section of the beam was estimated to be 6.5 mm. For response characterization as a function of intensity, the beam was mechanically chopped at the intermediate focus between two identical paraboloidal reflectors. The total power which arrived at the detector plane was measured with a calibrated detector. All measurements—detection, total power, and intensity, at 1.6, 4.3, and 9.8 THz—were performed using the same beam propagation distances to account for absorption by air. In this case, we investigated the behavior of CMOS TeraFETs. They were fabricated by a commercial 90-nm silicon CMOS process of United Microelectronics Corporation (UMC). A single-transistor layout was chosen in contrast to our previous double-FET designs.^{6,9,28,29} THz radiation was coupled to the drain terminal of the FET by an integrated patch antenna whose size was chosen to be resonant to the respective THz frequency. For each frequency, we used a separate device (three in this study). The NEP of the devices was $63 \text{ pW}/\sqrt{\text{Hz}}$ at 2.52 THz and $110 \text{ pW}/\sqrt{\text{Hz}}$ at 4.25 THz.³⁰

In order to check for the linearity of the detector response and deviations thereof, we measured the dependency of the rectified voltage on the incident THz radiation power. Data for the case of the Ti:sapphire-based source and the AlGaIn/GaN detector are exhibited in Fig. 1(a). The power of the THz pulses emitted from the photoconductive antenna was controlled by the antenna bias voltage. The measurements were made in the regime where the radiated power has a quadratic dependency on the generated photocurrent and the slope of the power versus applied antenna voltage is constant (the linearity as a function of antenna voltage was tested using electro-optic detection). The rectified signal of the TeraFET was found to depend linearly on THz power for a wide range of applied gate-bias voltages (see the figure inset for two exemplary voltage response curves as a function of gate bias). However, in the sub-threshold bias regime (threshold voltage $V_{th} = -0.98 \text{ V}$), there is clear evidence for a super-linear sensitivity to THz power. The main panel of Fig. 1(a) compares the power dependence at two gate bias voltages. At -0.7 V , above threshold, the dependence is linear, while it is nearly quadratic at -1.2 V (at other sub-threshold bias voltages, different exponents are found). The super-linearity of the response corroborates the findings of Ref. 20.

A pronounced super-linear response to high THz intensities was also obtained for the CMOS TeraFETs exposed to FEL radiation. The main panel of Fig. 1(b) presents the intensity dependence of the rectified voltage of a TeraFET exposed to radiation at 4.3 THz, for two gate voltages: one (0.5 V) chosen to be above and the other (0.2 V) below the transistor's threshold voltage of 0.37 V. As for the AlGaIn/GaN TeraFET, we find linear intensity dependence above threshold and a super-linear one below. For the gate voltage of 0.2 V of the main panel, a nearly quadratic dependence is observed. Deeper into the sub-threshold regime, the exponent becomes larger (see the figure inset); at zero gate bias, the response is proportional to the fourth power of the beam intensity. Note that at the highest time-averaged intensity $\langle I_{\text{THz}} \rangle$ of $7.5 \text{ mW}/\text{cm}^2$ of the main panel, one can discern the onset of saturation for both gate bias voltages. The super-linear regime is hence clearly distinct from the saturation regime where the autocorrelation measurements of Ref. 19 have been performed. We also note that one can calculate the onset of saturation to set in at a *peak* intensity I_{THz}^{pk} of about $55 \text{ W}/\text{cm}^2$. This value can be contrasted with the I_{THz}^{pk} of a few tens of kW/cm^2 required to reach saturation in transistors without antenna coupling.²⁰ The much lower saturation threshold of our measurements can largely be attributed to the efficient radiation coupling with the integrated antenna.

Having observed super-linear behavior with both AlGaIn/GaN HEMTs and CMOS FETs, we conclude that the phenomenon is universal and not dominated by the specific material system. For both types of FETs, the super-linear behavior occurs at gate bias voltages below the region of maximal responsivity. With the help of the established device models, one can show that both the super-linearity of the responsivity and the saturation behavior are primarily a consequence of the gate

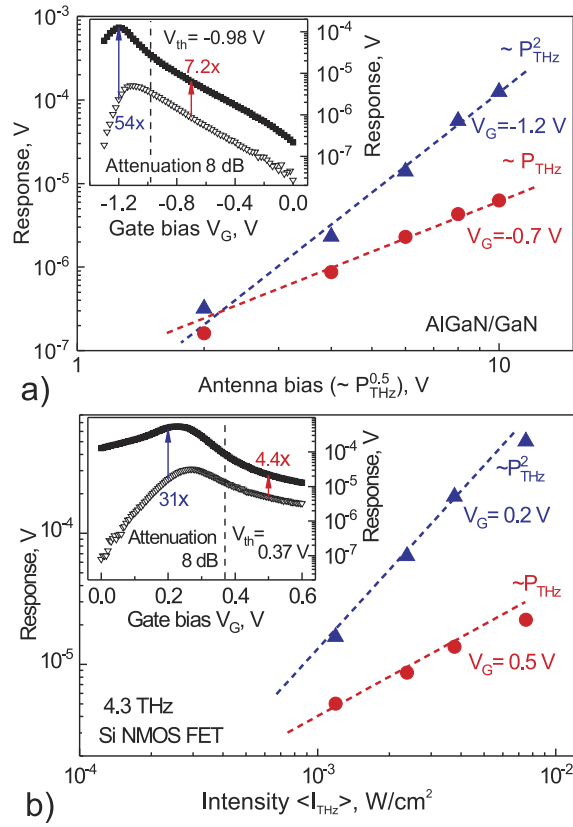


FIG. 1. (a) Rectified voltage of the AlGaIn/GaN TeraFET detector exposed to broad-band pulsed THz radiation as a function of THz field strength (expressed in terms of the bias voltage across the emitter) for two gate bias voltages: -0.7 V (red circles and dashed line guide to the eye) and -1.2 V (blue triangles and dashed line). Inset: rectified voltage as a function of the transistor's gate bias voltage for two THz power levels (the total beam power being unknown). The vertical dashed line indicates the turn-on threshold voltage of the HEMT. The vertical arrows annotated with the factors $54\times$ and $7.2\times$ indicate the enhancement of the rectified voltage at the given FET bias points when the THz beam power is increased by 8 dB. (b) Rectified voltage of a CMOS TeraFET detector exposed to narrow-band pulsed THz radiation (4.3 THz, FEL radiation) as a function of measured time-averaged THz intensity for two gate bias voltages: 0.5 V (red circles and dashed line guide to the eye) and 0.2 V (blue triangles and dashed line). Inset: rectified voltage as a function of the transistor's gate bias voltage for two THz power levels. Dashed line: turn-on threshold voltage of the FET. The vertical arrows annotated with the factors $31\times$ and $4.4\times$ indicate the enhancement of the rectified voltage at the given FET bias points when $\langle I_{\text{THz}} \rangle$ is increased by 8 dB starting from an intensity of 1.2 mW/cm 2 .

voltage dependence of the carrier density in the transistor channel. For the illustration, we can take a lumped-element FET picture. Let us apply an oscillating voltage V_D onto the drain setting source terminal to the ground and bias the gate with V_G below the threshold voltage V_{th} . Rectified current $I_D = G_{ch} \cdot V_D$ will come from the mixing terms in the product of drain voltage and modulated channel conductance $G_{ch} = 1/R_{ch} \propto \ln[1 + 1/2 \cdot \exp((V_G - V_{th} - V_D)/\eta V_T)]$. Here η is the nonideality factor and V_T is the thermal voltage. Whereas this simplified approach allows getting a qualitative understanding for nonlinear behavior of rectification when the amplitude of oscillating signal V_D becomes higher than a product ηV_T , excitation with frequencies exceeding transistor's cut-off frequency f_T requires using more sophisticated analysis. Therefore, we implemented both the standard non-quasi-static FET model³¹ and the distributed transistor model⁹ in the Advanced Design System (ADS) software environment of Keysight Technologies.³² A constant carrier mobility and a constant non-ideality factor (value of 2) have been assumed. Pulsed excitation was simulated as a waveform having one to several periods of oscillations at a fundamental frequency of 1 THz. The envelope solver was used to study the response dynamics within a time window of 40 ps. Results for the current responsivity (i.e., rectified current divided by the squared THz field amplitude) are presented in Fig. 2. For low excitation amplitudes, the current responsivity is constant at all gate bias values as expected for a

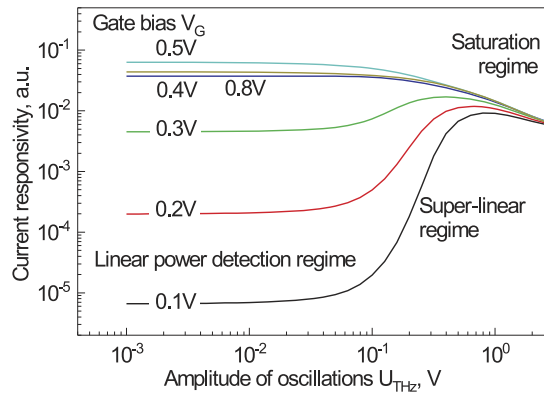


FIG. 2. Calculated current responsivity for pulsed excitation of a field-effect-transistor modeled with Keysight ADS. For an excitation amplitude not exceeding a few ten mV, the response is linearly proportional to the input power at all gate bias values. At a higher excitation amplitude, the response can either be super-linear or show saturation. Threshold voltage $V_{th} = 0.38$ V.

square-law (power) detector. For a bias above the threshold voltage, rectification at large field amplitudes results in saturation behavior as reported in the literature.^{17,19,20} However, in a sub-threshold bias regime, excitation with THz voltages coupled to the channel U_{THz} exceeding approximately 100 mV (or more precise—the thermal voltage times the nonideality-factor ηV_T) results in a strong super-linearity which is gate-bias-dependent. The model indicates that the dynamic range for this phenomenon is not very large and extends over just one to two orders of magnitude before saturation comes into play. Although it is not commonly reported, a super-linear response to high THz intensities was also recently predicted for Schottky diode detectors.³³

We finally show that the observed nonlinear dependency has practical applications for the measurement of the duration of THz pulses. Whereas for Fourier-transform-limited pulses, any linear power detector can be employed to determine the pulse duration from an interferogram of a pulse with its time-delayed replica (first-order autocorrelation), this does not apply for chirped pulses, where nonlinear detectors employing, for example, two-photon detection¹ or saturation of rectification¹⁹ must be used to measure the second-order autocorrelation. Following the latter route, we constructed a Michelson-type interferometer and measured interference patterns by adjusting the time delay between the two arms. Figure 3(a) presents interferograms measured with FEL radiation at 4.3 THz using the CMOS TeraFET as the detector. We chose three different gate bias values corresponding to the three different response conditions: a super-linear response (gate value: 0.1 V), linear response (0.3 V), and saturation (0.6 V). The smooth lines (in red color) in each plot are the results of fast delay scans representing higher-order autocorrelations (existing only in the non-linear response regimes, hence vanishing for the gate bias of 0.3 V). The fact that the FWHM of the fringe-resolved patterns (in blue color) and that of the higher-order autocorrelation curves are nearly equal shows that the chirp of the THz pulse is weak. Therefore, the field autocorrelation trace obtained for a gate voltage $V_G = 0.3$ V can be used to determine the pulse duration. Assuming a Gaussian waveform, the FWHM width $T_{1/2}$ of the interferogram yields a pulse duration of $T_{1/2}/(2\sqrt{\ln 2}) \approx 11.5$ ps. If the gate is biased at 0.2 V (data not shown), the detector signal is proportional to the power squared [see Fig. 1(b)] allowing us to use the same estimation procedures for the pulse duration as for intensity autocorrelators, i.e., $T_{1/2}/\sqrt{2} \approx 11.7$ ps.

While all three response regimes allow for interferometric autocorrelation measurements, the modulation depth is by far the largest in the super-linear regime. In that sense, this regime is better suited for pulse characterization than the saturation regime.^{19,34,35} For standard quadratic detection, in the case of interferometric autocorrelation, a ratio of 8:1 is expected between the signals measured for zero time delay and for temporally separated pulses. For an intensity autocorrelation, this ratio is 3:1.¹ Comparing with the measured data of the top panel of Fig. 3—recorded in the super-linear responsivity regime—one finds that the interferometric autocorrelation trace (blue line) exhibits a 7:1 ratio, whereas the intensity autocorrelation trace (red line) yields a 3:1 ratio. These values nearly correspond to those expected for quadratic detection, although the power dependence of the

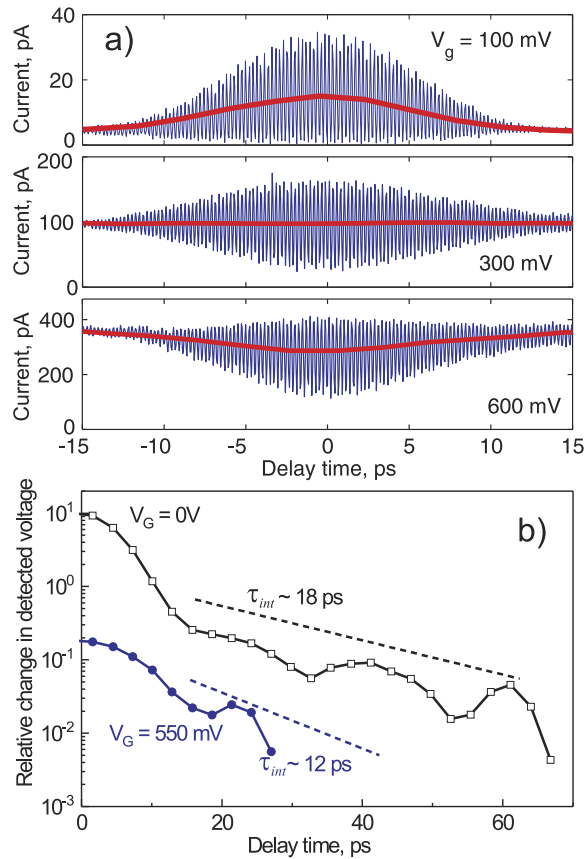


FIG. 3. (a) Two-pulse autocorrelation signals of FEL radiation at 4.3 THz recorded at different gate bias values. Data were recorded using fine-resolution time delay scanning (blue curves) and time-averaging fast scanning (red curves). Lock-in detection in the current mode. (b) Logarithmic plot of the absolute value of the rectified voltage as the function of delay time between two 4.3 THz pulses at two different gate bias values. The constant (incoherent) part is subtracted. Lock-in detection in the voltage mode.

responsivity is cubic at the given gate voltage. These ratios can be reproduced assuming given power dependencies and the intensity ratio of 1:5 between the different interfering arms. At zero gate bias, the measured intensity autocorrelation trace (data not shown) exhibits a 12:1 ratio due to the strong nonlinearity of the responsivity [see the inset of Fig. 1(b)].

The data of Fig. 3(a) and additional ones at other gate bias voltages also allow us to estimate the gate voltage dependence of the intrinsic response time (τ_{int}) of the transistor. While the transistor is sensitive to very high THz frequencies, the build-up of the full rectified signal as well as its decay is linked to the equilibration (mainly via diffusion) of the spatial charge carrier distribution. If τ_{int} is larger than the duration of the THz pulses used in the intensity autocorrelation measurements, the decay of that signal for large time delay should be determined by τ_{int} . In other words, outside the time window where interference occurs, the trailing THz pulse probes the disturbance of the charge carrier distribution in the channel introduced by the leading THz pulse. Evaluating intensity autocorrelation data recorded at gate bias voltages from 0 V to 0.6 V for large delay times [see Fig. 3(b)], we observe a signal decay which changes from 18 ps in the sub-threshold regime to about 12 ps (i.e., fully convolved with probing pulse duration) above the threshold. Contending ourselves with the general trend and omitting a deconvolution of the autocorrelation trace to take into account the THz pulse duration, we note that our estimates for τ_{int} fairly well agree with theory³⁶ predicting that the intrinsic response time of FETs fabricated in CMOS technology (with a mobility of about 200 cm²/V s) should be about 20 ps. The autocorrelation measurement hence allows an independent determination of the gate-voltage-dependent τ_{int} avoiding the limitations of read-out electronics.³⁷

Given this response speed, the TeraFET devices can conveniently be employed also for direct, non-interferometric characterization of THz pulses if a time resolution on the scale of ten picoseconds is sufficient.^{16,38} Examples are mode-locked THz quantum cascade lasers or Q-switched THz optical parametric oscillators.

In summary, we have presented experimental evidence for a super-linear response of FET-based THz detectors in the sub-threshold bias regime, when exposed to sufficiently strong THz radiation. We conclude that the super-linear response is a universal phenomenon and should be observable in all types of FETs when the amplitude of the radiation at the transistor terminal exceeds the thermal voltage (several tens of mV at room temperature). We have employed the nonlinearity for a determination of the intrinsic response speed of the detector as well as for the measurement of the duration of pulsed THz radiation.

The Vilnius team acknowledges the Research Council of Lithuania for financial support under Contract No. S-LAT-17-3. The Frankfurt team acknowledges partial financial support by the Hessian excellence initiative LOEWE, project “Sensors towards THz,” and the SAW Project No. SAW-2014-FBH-1 334 TSPiG of the Leibniz Society. Lithuanian-French cooperation was supported through the GILBERT program. The authors would like to express their thanks to Adam Ramer, Serguei Chevtchenko, and Wolfgang Heinrich from the Ferdinand-Braun-Institut (Berlin, Germany) for their help with the design and fabrication of the AlGaIn/GaN detector which was employed in this study. D..C. and V.K. are further grateful for partial financial support in the frame of the Marie Curie European Training Networks ITN CELTA, Contract No. 675683.

- ¹ H. Schneider, O. Drachenko, S. Winnerl, M. Helm, and M. Walther, *Appl. Phys. Lett.* **89**, 133508 (2006).
- ² H. Schneider, O. Drachenko, S. Winnerl, M. Helm, T. Maier, and M. Walther, *Infrared Phys. Technol.* **50**, 95 (2007).
- ³ S. Komiyama, *IEEE J. Sel. Top. Quantum Electron.* **17**, 54 (2011).
- ⁴ M. Dyakonov and M. Shur, *IEEE Trans. Electron Devices* **43**, 380 (1996).
- ⁵ I. Khmyrova and Y. Seijyou, *Appl. Phys. Lett.* **91**, 143515 (2007).
- ⁶ A. Lisauskas, U. Pfeiffer, E. ojefors, P. H. Bolivar, D. Glaab, and H. G. Roskos, *J. Appl. Phys.* **105**, 114511 (2009).
- ⁷ E. ojefors, U. R. Pfeiffer, A. Lisauskas, and H. G. Roskos, *IEEE J. Solid-State Circuits* **44**, 1968 (2009).
- ⁸ S. Preu, S. Kim, R. Verma, P. G. Burke, M. S. Sherwin, and A. C. Gossard, *J. Appl. Phys.* **111**, 024502 (2012).
- ⁹ S. Boppel, A. Lisauskas, M. Mundt, D. Seliuta, L. Minkevicius, I. Kaalynas, G. Valusis, M. Mittendorff, S. Winnerl, V. Krozer, and H. G. Roskos, *IEEE Trans. Microwave Theory Tech.* **60**, 3834 (2012).
- ¹⁰ G. R. Aizin and G. C. Dyer, *Phys. Rev. B* **86**, 235316 (2012).
- ¹¹ A. Lisauskas, M. Bauer, A. Ramer, K. Ikamas, J. Matukas, S. Chevtchenko, W. Heinrich, V. Krozer, and H. G. Roskos, in *2015 International Conference on Noise and Fluctuations (ICNF)*(IEEE, Xian, People’s Republic of China, 2015), pp. 1–5.
- ¹² A. Gutin, V. Kachorovskii, A. Muraviev, and M. Shur, *J. Appl. Phys.* **112**, 014508 (2012).
- ¹³ A. Gutin, T. Ytterdal, V. Kachorovskii, A. Muraviev, and M. Shur, *IEEE Sens. J.* **13**, 55 (2013).
- ¹⁴ S. Preu, H. Lu, M. S. Sherwin, and A. C. Gossard, *Rev. Sci. Instrum.* **83**, 053101 (2012).
- ¹⁵ S. Preu, M. Mittendorff, S. Winnerl, H. Lu, A. C. Gossard, and H. B. Weber, *Opt. Express* **21**, 17941 (2013).
- ¹⁶ D. Vo, W. Zouaghi, M. Jamshidifar, S. Boppel, C. McDonnell, J. R. P. Bain, N. Hempler, G. P. A. Malcolm, G. T. Maker, M. Bauer, A. Lisauskas, A. Ramer, S. A. Shevchenko, W. Heinrich, V. Krozer, and H. G. Roskos, *J. Infrared, Millimeter, Terahertz Waves* **39**, 262 (2017).
- ¹⁷ D. B. But, C. Drexler, M. V. Sakhno, N. Dyakonova, O. Drachenko, F. F. Sizov, A. Gutin, S. D. Ganichev, and W. Knap, *J. Appl. Phys.* **115**, 164514 (2014).
- ¹⁸ S. Rudin, G. Rupper, A. Gutin, and M. Shur, *J. Appl. Phys.* **115**, 064503 (2014).
- ¹⁹ S. Preu, M. Mittendorff, S. Winnerl, O. Cojocari, and A. Penirschke, *IEEE Trans. Terahertz Sci. Technol.* **5**, 922 (2015).
- ²⁰ N. Dyakonova, P. Faltermeier, D. B. But, D. Coquillat, S. D. Ganichev, W. Knap, K. Szuklarek, and G. Cywinski, *J. Appl. Phys.* **120**, 164507 (2016).
- ²¹ J. Joh and J. A. del Alamo, *IEEE Trans. Electron Devices* **58**, 132 (2011).
- ²² M. Baillergeau, K. Maussang, T. Nirrengarten, J. Palomo, L. H. Li, E. H. Linfield, A. G. Davies, S. Dhillon, J. Tignon, and J. Mangeney, *Sci. Rep.* **6**, 24811 (2016).
- ²³ P. J. Hale, J. Madeo, C. Chin, S. S. Dhillon, J. Mangeney, J. Tignon, and K. M. Dani, *Opt. Express* **22**, 26358 (2014).
- ²⁴ A. Dreyhaupt, S. Winnerl, T. Dekorsy, and M. Helm, *Appl. Phys. Lett.* **86**, 121114 (2005).
- ²⁵ S. A. Chevtchenko, F. Brunner, J. Wurfl, and G. Trankle, *Phys. Status Solidi A* **207**, 1505 (2010).
- ²⁶ M. Bauer, A. Ramer, S. Boppel, S. Chevtchenko, A. Lisauskas, W. Heinrich, V. Krozer, and H. G. Roskos, in *10th European Microwave Integrated Circuits Conference (EuMIC), September 07–08, 2015* (IEEE, Paris, France, 2015), pp. 1–4.
- ²⁷ S. Boppel, M. Ragauskas, A. Hajo, M. Bauer, A. Lisauskas, S. Chevtchenko, A. Ramer, I. Kaalynas, G. Valusis, H.-J. Wurfl, W. Heinrich, G. Trankle, V. Krozer, and H. G. Roskos, *IEEE Trans. Terahertz Sci. Technol.* **6**, 348 (2016).
- ²⁸ S. Boppel, A. Lisauskas, A. Max, V. Krozer, and H. Roskos, *Opt. Lett.* **37**, 536 (2012).
- ²⁹ A. Lisauskas, S. Boppel, M. Mundt, V. Krozer, and H. G. Roskos, *IEEE Sens. J.* **13**, 124 (2013).
- ³⁰ M. Bauer, R. Venckevičius, I. Kaalynas, S. Boppel, M. Mundt, L. Minkevicius, A. Lisauskas, G. Valusis, V. Krozer, and H. G. Roskos, *Opt. Express* **22**, 19235 (2014).
- ³¹ A. Roy, J. Vasi, and M. Patil, *IEEE Trans. Electron Devices* **50**, 2393 (2003).

- ³² M. Bauer, S. Boppel, J. Zhang, A. Ramer, S. Chevtchenko, A. Lisauskas, W. Heinrich, V. Krozer, and H. G. Roskos, [Int. J. High Speed Electron. Syst.](#) **25**, 1640013 (2016).
- ³³ E. R. Brown, S. Sung, W. S. Grundfest, and Z. D. Taylor, [Proc. SPIE](#) **8941**, 89411E (2014).
- ³⁴ X. Cai, A. B. Sushkov, R. J. Suess, M. M. Jadidi, G. S. Jenkins, L. O. Nyakiti, R. L. Myers-Ward, S. Li, J. Yan, D. K. Gaskill, T. E. Murphy, H. D. Drew, and M. S. Fuhrer, [Nat. Nanotechnol.](#) **9**, 814 (2014).
- ³⁵ M. Mittendorff, S. Winnerl, J. Kamann, J. Eroms, D. Weiss, H. Schneider, and M. Helm, [Appl. Phys. Lett.](#) **103**, 021113 (2013).
- ³⁶ S. Rudin, G. Rupper, and M. Shur, [J. Appl. Phys.](#) **117**, 174502 (2015).
- ³⁷ S. Regensburger, M. Mittendorff, S. Winnerl, H. Lu, A. C. Gossard, and S. Preu, [Opt. Express](#) **23**, 20732 (2015).
- ³⁸ K. Ikamas, A. Lisauskas, S. Boppel, Q. Hu, and H. G. Roskos, [J. Infrared, Millimeter, Terahertz Waves](#) **38**, 1183 (2017).